Use of rapid prototyping technology in complex plastic structures
Part I. Bench testing and numerical calculations of deformations in harmonic drive made from ABS copolymer

Jacek Pacana[1), *)], Rafał Oliwa[2)]

DOI: dx.doi.org/10.14314/polimery.2019.1.7

Abstract: In the study, measurements of 3D deformations of the flexspline in harmonic drive were performed by applying a digital image correlation (DIC) method. The tests were carried out with the use of physical 3D printed models made of ABS copolymer (acrylonitrile-butadiene-styrene), which ensured sufficient capacity and rigidity of the structures. The findings related to deformations in flexspline, obtained through bench testing, were compared to the results of calculations conducted using the finite element method (FEM). Significant convergence in the findings obtained using the two methods was shown, yet deformations measured in the real-life model were characterized by greater irregularity compared to the corresponding solutions obtained with the numerical method. The results obtained through optical measurement confirm that physical models made of plastics, built using rapid prototyping technology, can justifiably be applied in bench testing of prototype gear transmissions.

Keywords: harmonic drive, Aramis 3D, optical deformation measurement, FEM, flexspline, ABS, 3D printing.

Zastosowanie technologii szybkiego prototypowania skomplikowanych konstrukcji z tworzyw polimerowych
Cz. I. Badania stanowiskowe oraz obliczenia numeryczne odkształceń przekładni falowej otrzymanej z kopolimeru ABS

Streszczenie: Z wykorzystaniem metody cyfrowej korelacji obrazu (DIC) przeprowadzono pomiary odkształceń 3D koła podatnego zębatej przekładni falowej. Badania wykonano przy użyciu modeli fizycznych wytworzonych z zastosowaniem druku 3D z kopolimeru ABS, zapewniającego wystarczającą nośność i sztywność modelu. Uzyskane w badaniach stanowiskowych wartości odkształceń koła podatnego porównano z wynikami obliczeń przeprowadzonych z zastosowaniem metody elementów skończonych (MES). Wykazano dużą zbieżność otrzymanych wyników, jednak odkształcenia zmierzone na modelu rzeczywistym charakteryzują się większą nieregularnością niż odpowiadające im rozwiązania uzyskane metodą numeryczną. Wyniki otrzymane w pomiarach optycznych wskazują na zasadność stosowania w badaniach stanowiskowych prototypów przekładni zębatych modeli fizycznych wykonanych z tworzyw polimerowych z wykorzystaniem technologii szybkiego prototypowania.

Słowa kluczowe: zębata przekładnia falowa, Aramis 3D, optyczne pomiary deformacji, MES, koło podatne, ABS, drukowanie 3D.

Engineering calculations frequently apply numerical analyses, based on the finite elements method (FEM). The use of such analyses in combination with state-of-the-art CAx software allows to design even highly advanced structures. However, despite the high effectiveness of computer-aided calculations, one has to remember that they introduce simplifications and are based on discrete models. Therefore, whenever it is possible, numerical so-

[1)] Rzeszow University of Technology, Faculty of Mechanical Engineering and Aeronautics, Department of Mechanical Engineering, Al. Powstańców Warszawy 8, 35-959 Rzeszów, Poland.

[2)] Rzeszów University of Technology, Faculty of Chemistry, Department of Polymer Composites, Al. Powstańców Warszawy 6, 35-959 Rzeszów, Poland.

[*)] Author for correspondence; e-mail: pacanaj@prz.edu.pl

lutions should be verified by means of analytic or experimental methods [1–3].

Even if limited to selected results of numerical analysis, critical assessment and comparison to other results make it possible to identify potential errors which frequently are decisive for the strength of the entire structure. Analytic calculations may be applied to inspect the simplest cases, yet the use of general definitions and formula is insufficient in more complex tasks. In many cases in order to accurately verify calculations it is necessary to conduct experimental tests with the use of functional prototypes or finished products [4, 5]. Although they require significantly larger resources, even the simplest bench tests allow for greater certainty regarding the findings, and they enable verification of results of numerical calculations [6, 7].

In order to improve effectiveness of experiments and to reduce their costs, they are carried out with the use of prototypes made of polymer materials. Functional models for bench testing are more and more often built using rapid prototyping (RP) methods [8, 9]. These methods permit the use of materials with greatly varied properties; additionally, these materials may be further modified [10], therefore the scope of the tests may be very broad. Conclusions based on experiments involving models built using RP methods provide a lot of indispensable information to be applied in designing new and enhanced structures. Experiments are frequently conducted in combination with other calculation and measurement methods, which additionally increases accuracy of the final conclusions [11–13].

Harmonic drive is an example of a highly intricate structure, with extremely complex performance characteristics [14, 15]. In this case it is difficult to analytically determine the final strength of the structure. During the operation the most loaded element, *i.e.*, the flexspline is deflected along multiple planes by the generator, and at the same time strained by the transfer of torque, and it remains in multi-pair contact with the rigid ring. Some research publications present a method for calculating each of the characteristic loads separately, since overall calculations would be too complicated. This is why numerical methods, mainly FEM, are applied in the process of designing harmonic drives [16]. By using detailed solid models and at the same time simulating the loads and movement of the elements, it is possible to accurately map the conditions during operation of the gearing. The obtained findings are presented mainly in a form of strain maps for the models of the relevant gearings, or as graphs for selected cross-sections.

EXPERIMENTAL PART

Materials

In the study, paddle-shaped specimens as well as the prototype harmonic drive were made from ABS filament, provided by Hbot3D Filaments company.

Preparation of samples for testing

The paddle-shaped specimens designed for materials testing were 3D printed, with the use of UP! Plus 2 printer, from TierTime, and parameter settings listed in Table 1. Solid fill was applied, and the direction of fibers in the specimens was consistent with the direction of tension affecting them. This corresponded with the arrangement of the consecutive 3D print layers on the models of the gears examined.

T a b l e 1. Basic technical parameters of UP! Plus 2 printer

Parameter	Value
Print bed size, mm	140 × 140
Maximum model height, mm	135
Nozzle size, mm	0.4
Layer thickness, mm	0.15
Printing temperature of ABS, °C	250
Filament diameter, mm	1.75
Printing method	MEM

The building blocks of the harmonic drive were also 3D printed, using the same forming design. The relevant harmonic drive had the following parameters of the toothed rims: module – 0.7 mm, number of teeth in the flexspline – 120, number of teeth in the rigid ring – 122. The dimensions of the flexspline were as follows: outer diameter 96.7 mm, total length 70 mm. The rapid prototyping method greatly facilitated, and made it possible to speed up, the process of preparing the elements of the gearing. Being an additive method, 3D printing was particularly advantageous in the case of the flexspline, designed as a thin-walled barrel with small-module toothed rim. Conventional removal processing applied in manufacturing of such elements requires special equipment and is linked with significant technological challenges. In the case of the relevant 3D printing technique the material is applied in layers, and no additional machining stress occurs during construction of the model, which greatly facilitates the entire process [17, 18].

Methods of testing

Gear deformation analysis

Deformations in a functional prototype of harmonic drive made from ABS copolymer [19, 20] were examined at a specially designed test station, whose layout is presented in Fig. 1.

In its structure, the station included a generator driver shaft, a rigid ring housing, as well as bearing support and housings which were made of steel, in order to ensure high rigidity of the test station. Deformations of the flexspline were determined with the use of digital image correlation (DIC) method and Aramis 3D system from

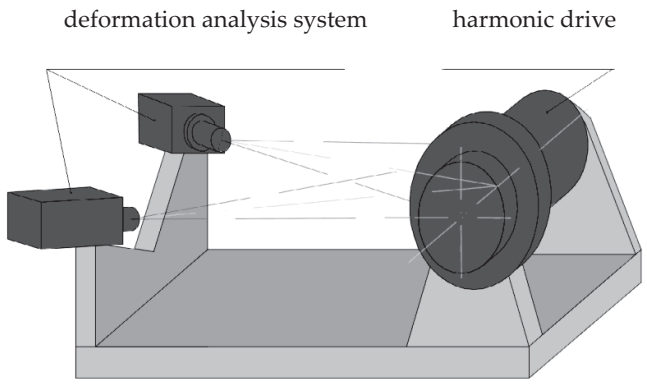

Fig. 1. Layout of test station designed in accordance with a deformation analysis system

GOM GmbH. The applied measuring system consists of two cameras which record correlated high resolution images. Coordinates of points located on the surface of the model are determined with the use of triangulation. Based on the measurement data from the system it is possible to determine material properties, analyze motion of objects, and classify finished products according to geometric criteria. The complete test station comprised the studied harmonic drive, deformation analysis system (Fig. 2), and a computer designed to operate the devices and to record the results.

Before the measurements, a pattern with a characteristic distribution of points was applied to the surface of the ring; based on that a spatial image of the relevant element was created. The model of the flexspline of the harmonic drive, ready for measurements, with the stochastic distribution of points on the outer surface, is presented in Fig. 3.

Prepared this way, the functional prototype was mounted onto the test station to enable precise measurements of flexspline deformations during operation. Flexspline deformations in the harmonic drive were measured multiple times, under the same ambient conditions and with a constant setting of the test station. By repeating the measurement cycle it was possible to acquire detailed results and to avoid random errors. All the results, in a form of images, were saved and catalogued by the computer connected to Aramis 3D system. For each measurement first of all a baseline image of the relevant surface was recorded and the subsequent images were compared to it. Further operations took place in GOM Correlate software designed for processing of results obtained from an optical deformation analysis system.

Determination of material constants

Static tension test was performed to determine the properties of the material used in the construction of the prototype. The tests were carried out in conformity with ISO 527-1:1998, with the use of 3D printed paddle-shaped specimens. To define material constants, the digital image

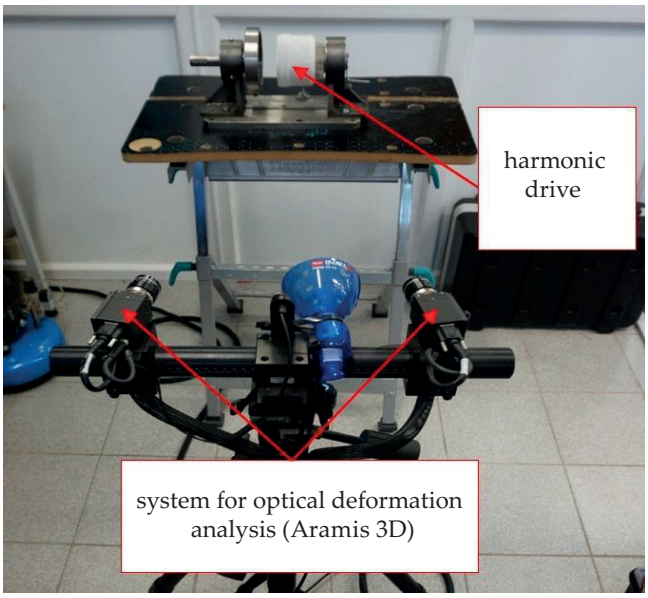

Fig. 2. View of the test station designed for optical deformation analysis

Fig. 3. Model of the flexspline, ready for optical measurements

correlation method based on Aramis system was again used, in combination with Instron 5967 tensile strength tester [21]. Given the fact that the findings of bench testing were to be compared with results of numerical calculations, it was important that the same input conditions be maintained in both methods; all the building blocks of the relevant harmonic drive were 3D printed, based on the same models which were used in FEM calculations. Therefore, it was only necessary to define properties of the material used in the construction of the prototype. To this end the applied polymer was subjected to static tension test. All the specimens were prepared following the procedure described earlier.

FEM numerical analysis

FEM calculations took into account material data obtained through static tension test, by applying the same model which was used in producing 3D prints. Computer simulations were conducted in Abaqus software.

RESULTS AND DISCUSSION

Determination of material constants

As a result of tension tests used in combination with the digital image correlation method, the data were obtained in a form of photographs showing areas of deflexion on the entire surface of the specimen during stretching. Analysis of the images made it possible to generate relations between strain and stress distribution, which were used to directly determine Young's modulus, maximum tensile stress and deformation as well as Poisson's ratio (Figs. 4, 5). Based on the analyses shear modulus was also determined by applying the equation utilizing the relationship between Young's modulus and Poisson's ratio for isotropic materials:

$$G = \frac{E}{2(1+\upsilon)} \tag{1}$$

where: E – Young's modulus [GPa], υ – Poisson's ratio.

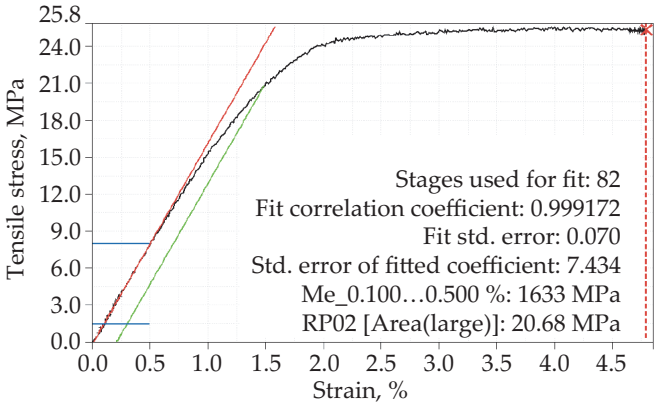

Fig. 4. Stress-strain diagram during tension test in a specimen

T a b l e 2. Mean values of the parameters in ABS material

Parameter	3D printing	Injection molding
Tensile strength (R_m), MPa	24.96	44
Strength at break (ε), %	4.70	9
Young's modulus (E), MPa	1581.83	2000
Poisson's ratio (υ)	0.38	0.34
Flexural modulus (G), MPa	573.39	900

The findings are presented in Table 2 and compared to the material properties listed in the relevant safety data sheet.

Material parameters determined for the 3D printed paddle-shaped specimens differ from the values declared by the manufacturer of ABS. Tensile strength, Young's modulus and yield limit are visibly lower in the case of the 3D printed specimens (Table 2). The recorded images were analyzed in detail for axial strain ε_y, and transverse strain ε_x, and the respective values were presented in a graphic form in Figs. 6 and 7. The findings show significant ability of ABS polymer for deformations in the direction of Y and X axes. The maximum values of deformations in the direction of Y and X axes amount to 9 % and -3.5 %, respectively, while the mean values amount to 4.5 % and -1.7 %, respectively. The differences visibly increase after the yield limit has been exceeded.

Analysis of bench testing and FEM calculations

Given the fact that during the operation of harmonic drive, its flexspline is deformed by the impact of the generator, in order to verify FEM results the deformations were examined with the use of digital image correlation enabling measurement of the deformation in the outer surface of the flexspline. The obtained results were used to verify the numeric calculations related to the same harmonic drives.

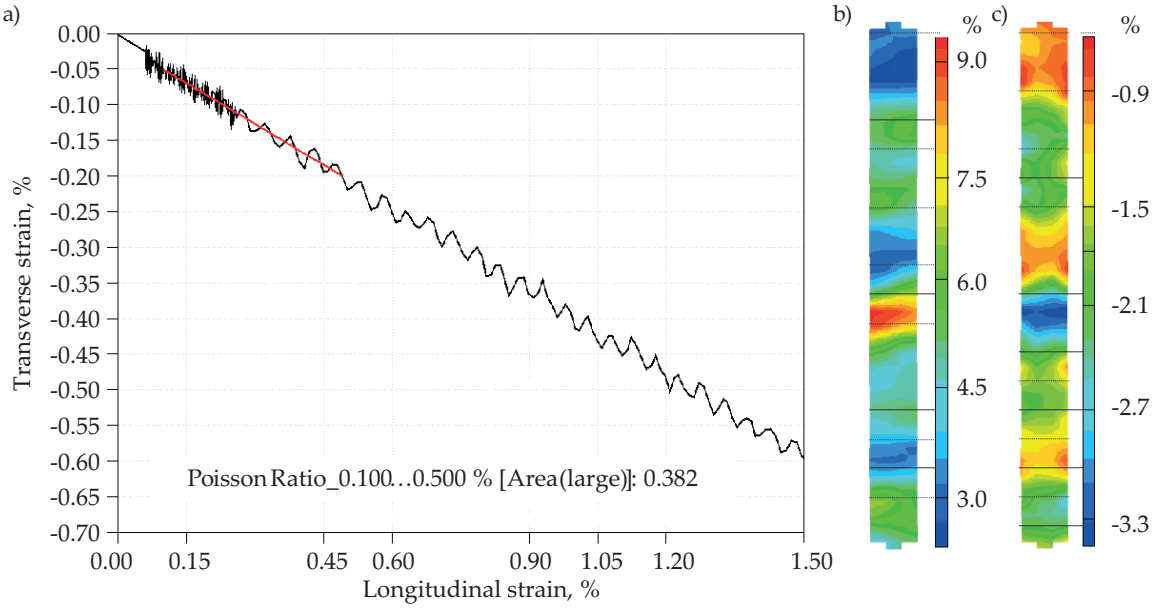

Fig. 5. Determination of Poisson's ratio: a) strain diagram, b) distribution of axial strains ε_y, c) distribution of transverse strains ε_x

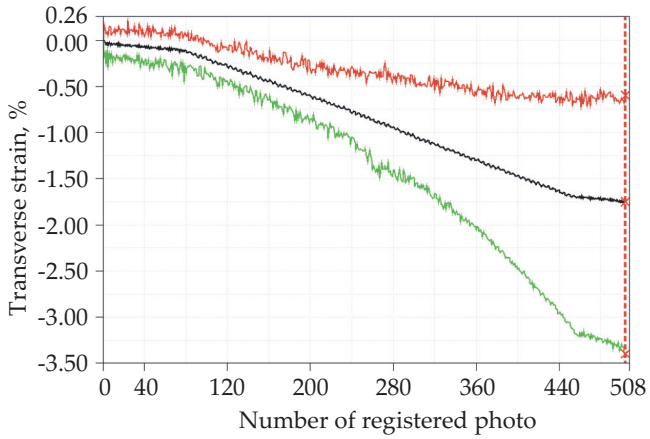

Fig. 6. Sample curve representing transverse strain ε_x

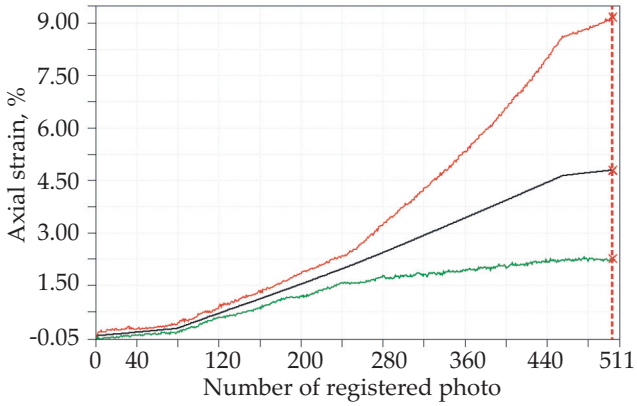

Fig. 7. Sample curve representing axial strain ε_y

Figure 8 shows the result of a measurement related to generator induced deformation of flexspline in the harmonic drive. The colored contour lines on the model surface represent different values of its deformation with respect to the baseline. The model does not comprise the entire flexspline because high quality results were possible only if the area was limited. The figure presents a situation in which the major axis of the generator is positioned horizontally, and oriented directly towards the cameras. In such alignment it is possible to observe the largest positive values of radial deflexion, which in Fig. 8 is represented by blue color. After the generator rotates by 90°, the position in front of the cameras will be occupied by the minor axis of the generator with displacements occurring towards the inside of the flexspline. In order to obtain results for the entire model, the measurements were carried out continuously during a complete rotation of the generator.

Correlate software

The surface obtained *via* optical measurement of the deformed flexspline model presents numerous errors in the toothed rim. This is caused by incorrect mapping of the very small tooth surfaces, because resolution was defined in such a way as to obtain high quality results for the flexspline body. Apart for the toothed rim the results are legible and may be used to verify numerical calculations. Figure 9 presents the results of computer-aided FEM calculations for the same model of flexspline in harmonic drive. The numerical calculations applied the strength parameters determined experimentally for ABS material during the tensile strength test. In FEM calculations it was possible to use complete models, therefore the results relating to both the major and the minor axis of the generator were determined in one model. The results based on the conducted simulations represented generator induced deformations in the model.

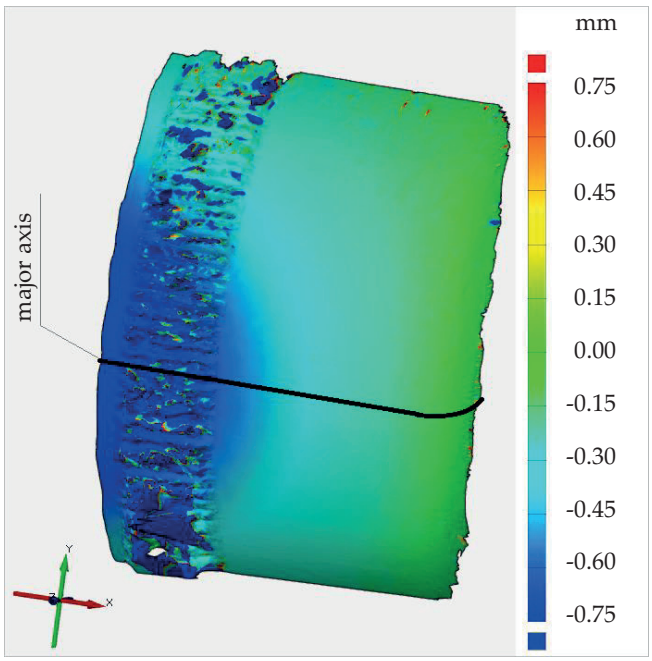

Fig. 8. Presentation of the results of flexspline deformation measurement in GOM

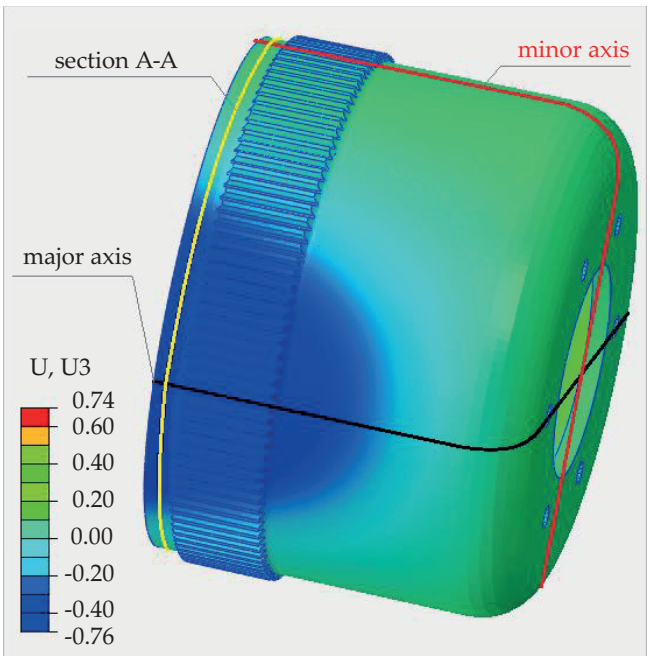

Fig. 9. Map of generator induced deformations on the flexspline surface, based on FEM calculations

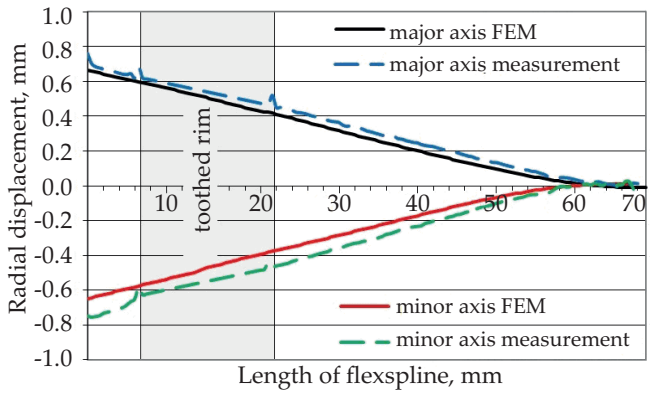

Fig. 10. Diagram showing radial displacements in model flexspline in selected longitudinal sections

A comparison of the findings acquired using optical measurements and numerical calculations shows a similarity in the distribution of deformation values in the outer flexspline surface. However, visual assessment of maps with model contour lines is not sufficiently accurate. Graphic representations of displacements along the major and minor axis of the generator were prepared to enable more precise conclusions. The diagram (Fig. 10) presents mean values of optical measurements and FEM analysis results retrieved from computational models. Due to the poor mapping of the toothed rim in the optical measurements, this part was disregarded in the analyses, and the relevant fragment in the graph was marked and replaced with a straight line.

While comparing the values of radial displacements identified by optical measurements and FEM calculations it is possible to notice a significant concurrence of these findings. Deformations of similar nature were identified in the entire length of the flexspline, along both the major and minor axis of the generator. However, the values of deformations measured for the real-life flexspline model were greater than the corresponding results of FEM calculations. Nevertheless, the differences between the findings obtained with the two methods amounted to 15 % at the most. These differences are linked with the fact that FEM calculations were based on ideal models, which did not account for manufacturing and assembly errors, inhomogeneity of materials and temperature induced effects.

The findings related to the functional prototype of the gearing make it possible to introduce correction in the numerical calculations to improve their accuracy. Following the adjustment it was established that actual deformation of the flexspline is greater than expected, and this should be taken into account in further numerical calculations related to flexspline in harmonic drive. Notably, to enable reading of the complete results for the flexspline, the element was mounted independently, without the cooperating rigid ring. This was done because the main purpose was to examine results for the entire length of the flexspline, to be obtained in the same conditions applied in both methods. The final conclusions may be transposed to the entire gearing, following the principles of model similarity [22]. Data acquired from Aramis 3D measuring system and FEM calculations were taken into account in comparative analysis of transverse strain in the flexspline, in Fig. 9 marked as A-A. Its position in the model was defined in such a way as to achieve the largest displacement values, and consequently show most clearly the differences between the two methods. In this experiment, in order to ensure real-life operating conditions for the harmonic drive, a complete prototype, *i.e.*, including a flexspline, was used in both FEM calculations and in optical measurements. The diagrams in Fig. 11 present resultant radial deformations occurring in a specific cross-section identified by optical measurement of flexspline deformed by cam generator, and the corresponding values determined in Abaqus software. The course of the diagrams in both cases is similar, yet it is possible to notice differences in the values for the specific cross-sections. The size of the deformation along the major and minor axis of the generator is usually greater for the measurements of real-life model than in the case of FEM calculations. Additionally, it can be observed that the real-life model is more rigid than the one adopted in numerical calculations. This is reflected by the greater width of the diagram related to optical measurements in the area of the minor axis. Here the generator does not adjoin the inner diameter of the flexspline, which is the case in the area of the major axis. The numerical calculations adopted a theoretical form of flexspline deformation, consequently the displacement diagram is more regular, consistent with relationships reported in the literature [8, 10].

Optical measurements performed using a system designed for surface deformation analysis again have shown that greater flexspline deformations occur in a real-life harmonic drive compared to those calculated with the use of FEM. Conclusions from the present study should be taken into account in future numerical calculations related to such structures.

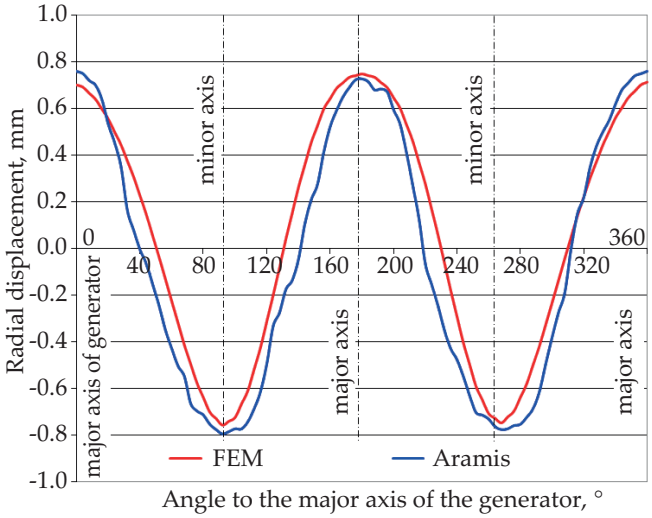

Fig. 11. Deformation along the perimeter of the flexspline, in a selected cross-section

CONCLUSIONS

During the process of designing such complicated structures as harmonic drive it is necessary to perform bench testing. Analytic calculations and numerical simulations are important tools supporting the design process. However, initial analyses based on numerical methods should subsequently be verified, experimentally if possible.

Hence, a novel test station was designed, built, and then applied to perform measurements of the flexspline in the harmonic drive, using an optical system of deformation analysis. Resulting from the adequate choice of materials used in elements of the harmonic drive, it was possible to produce the components by 3D printing. Harmonic drives as a rule are made of steel, but their flexsplines are frequently made of plastics (POM – polyoxymethylene, PC – polycarbonate) by injection molding. Such solutions are expensive and complicated in technological terms, and due to this they are mainly used in mass production. Consequently the use of harmonic drives is significantly limited, due to both their insufficient variability and the price. Given the above, it was reasonable to carry out tests confirming the viability of producing elements of this type with the use of 3D printing. The cost of producing the prototype gears using RP methods, for the needs of the present experiments, was dozens of times lower than if the elements were produced using conventional removal processing. During the tests it was observed that the physical models made of ABS are highly suitable for bench testing because the ways they are deformed and transmit the load correspond to the operation of standard mass-produced structures. Given the fact that harmonic drives as a rule are not subjected to heavy loads, it is reasonable to conclude that the use of 3D printing method would significantly facilitate and speed up production of harmonic drives, which would still satisfy necessary requirements for kinematic accuracy and carrying capacity. Further research, however, is needed to provide supporting evidence related to a wider range of parameters.

The analyses show that similar results were obtained from FEM calculations and in the case of real-life models. Yet, the measured values of flexspline deformation in most cases were slightly higher than the calculated values. This is associated with such factors affecting the gearing as slackness, inaccuracy of assembly, or kinematic errors, which are difficult to eliminate from such structures. Therefore it is necessary to consider these differences in future numerical calculations so that they more accurately reflect actual conditions of harmonic drives operation.

Experimental confirmation of the numerical findings shows that FEM calculations are highly effective and their use in engineering calculations is fully justified. The results of the optical measurements provide evidence for the high accuracy of 3D printed model flexsplines in harmonic drives, which suggests their viability for use in less demanding industrial applications.

REFERENCES

[1] „Przekładnie zębate o nietypowym zazębieniu – modelowanie, prototypowanie, badania stanowiskowe" (red. Markowski T.), Oficyna Wydawnicza Politechniki Rzeszowskiej, Rzeszów 2009.

[2] Sobolak M., Budzik G.: *Rapid Prototyping Journal* **2008**, *14*, 197. https://doi.org/10.1108/13552540810896148

[3] Kosmol J., Mnich M.: *Prace Naukowe Katedry Budowy Maszyn* **2013**, *2*, 49.

[4] Bernaczek J., Sobolewski B., Warchoł S.: *Mechanik* **2015**, *12*, 13. http://dx.doi.org/10.17814/mechanik.2015.12.548

[5] Budzik G., Sobolak M., Kozik B., Sobolewski B.: *Journal of KONES Powertrain and Transport* **2011**, *18* (4), 41.

[6] Li S.: *Mechanism and Machine Theory* **2016**, *104*, 1. https://doi.org/10.1016/j.mechmachtheory.2016.05.020

[7] Pacana J., Witkowski W., Mucha J.: *Strength of Materials* **2017**, *3*, 388.

[8] Farstad J.M., Netland Ø., Welo T.: *Procedia CIRP* **2017**, *60*, 247. https://doi.org/10.1016/j.procir.2017.02.009

[9] Krolczyk G., Raos P., Legutko S.: *Tehnički Vjesnik – Technical Gazette* **2014**, *21*, 217. UDC/UDK 620.191.083:621.941]:658.624

[10] Oleksy M., Budzik G., Heneczkowski M., Markowski T.: *Polimery* **2010**, *55*, 194.

[11] Budzik G.: „Dokładność geometryczna łopatek turbin silników lotniczych", Oficyna Wydawnicza Politechniki Rzeszowskiej, Rzeszów 2013.

[12] Tsai Y.C., Jehng W.K.: *Journal of Materials Processing Technology* **1999**, *95*, 169. https://doi.org/10.1016/S0924-0136(99)00287-3

[13] Gutiérrez S.C., Zotovic R., Navarro M.D., Meseguer M.D.: *Procedia Manufacturing* **2017**, *13*, 283. https://doi.org/10.1016/j.promfg.2017.09.072

[14] Mijał M.: „Synteza falowych przekładni zębatych", Oficyna Wydawnicza Politechniki Rzeszowskiej, Rzeszów 1999.

[15] Kayabasi O., Erzincanli F.: *Materials and Design* **2007**, *28*, 441. https://doi.org/10.1016/j.matdes.2005.09.009

[16] Ostapski W.: „Przekładnie falowe", Oficyna Wydawnicza Politechniki Warszawskiej, Warszawa 2011.

[17] Budzik G.: *Archives of Foundry Engineering* **2007**, *7* (2), 65. http://www.afe.polsl.pl/index.php/pl/magazine/cat/1/archives-of-foundry-engineering http://journals.pan.pl/dlibra/journal/96939

[18] Sobolak M., Jagiełowicz P.: *Czasopismo Techniczne. Mechanika* **2010**, *107*, 159. http://suw.biblos.pk.edu.pl/resourceDetails&rId=786

[19] Cader M., Oliwa R., Markowska O., Budzik G.: *Polimery* **2017**, *62*, 27. http://dx.doi.org/10.14314/polimery.2017.027

[20] Sasimowski E.: *Przetwórstwo Tworzyw* **2015**, *21* (4), 349. bwmeta1.element.baztech-7da3b67e-6b68-41f7-9ace--47fd09f599fc

[21] Oliwa R.: *Mechanik* **2015**, *12*, 147. http://dx.doi.org/10.17814/mechanik.2015.12.576

[22] Budzik G., Kozik B., Pacana J.: *Journal of KONES Powertrain and Transport* **2009**, *16* (2), 55.

Received 19 III 2018.